## S10-004

# Ca cofactor of the water-oxidation complex: Evidence for a Mn/Ca heteronuclear cluster

RM Cinco,[1,2] JH Robblee,[1,2] J Messinger,[1,3] C Fernandez,[1,2] KL McFarlane,[1] SA Pizarro,[1,2] K Sauer[1,2] and VK Yachandra[1]

[1]*Melvin Calvin Laboratory, Physical Biosciences Division, Lawrence Berkeley National Laboratory, Berkeley, CA 94720. Fax: 510 486 6059, e-mail: VKYachandra@lbl.gov*

[2]*Department of Chemistry, University of California, Berkeley, CA 94720-5230*

[3]*Max Volmer Laboratorium der TU Berlin, D-10623 Berlin, Germany*

*Keywords:* Mn complex, Ca cofactor, strontium, photosynthetic water oxidation, oxygen evolution, X-ray absorption spectroscopy

### Introduction

Calcium and chloride are necessary cofactors for the proper function of the oxygen-evolving complex (OEC) of Photosystem II (PS II). Located in the thylakoid membranes of green plants, cyanobacteria and algae, PS II and the OEC catalyze the light-driven oxidation of water into dioxygen (released into the biosphere), protons and electrons for carbon fixation. The actual chemistry of water oxidation is performed by a cluster of four manganese atoms, along with the requisite cofactors $Ca^{2+}$ and $Cl^-$ (Debus, 1992). While the Mn complex has been extensively studied by X-ray absorption techniques (XANES and EXAFS) (Robblee et al., 2001), comparatively less is known about the $Ca^{2+}$ cofactor. The fewer number of studies on the $Ca^{2+}$ cofactor have sometimes relied on substituting the native cofactor with strontium or other metals (Boussac & Rutherford, 1988; Debus, 1992), and have stirred some debate about the structure of the binding site. Past efforts using Mn EXAFS on Sr-substituted PS II are suggestive of a close link between the Mn cluster and Sr, within 3.5 Å (Latimer et al., 1995). The most recent published study using Sr EXAFS on similar samples confirms this finding of a 3.5 Å distance between Mn and Sr (Cinco et al., 1998). This finding was based on a second Fourier peak ('R' ~ 3 Å, Fig. 1) in the Sr EXAFS from functional samples, but is absent from inactive, hydroxylamine-treated PS II. This Fourier peak II was found to fit best to two (2) Mn at 3.5 Å rather than lighter atoms (carbon). Nevertheless, other experiments have given contrary results (Riggs-Gelasco et al., 1996).

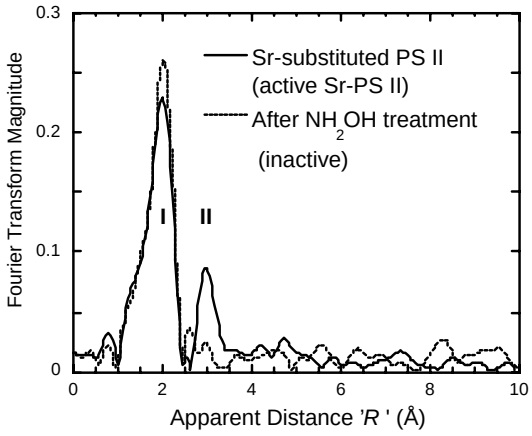


**Fig. 1**. Fourier Transform of Sr EXAFS from isotropic Sr-substituted PS II samples ($k^3$-weighted, $k$ = 2.7 – 11.7 Å$^{-1}$). The active Sr-PS II (solid line) is the average of 99 scans and the inactive sample (dashed line) is the average of 113 scans. Fourier peak I consists of nearest-neighbor oxygen atoms while peak II fits best to Mn scattering atoms. '*R*' is less than the actual distance by about 0.5 Å.

We wanted to extend the technique by using polarized Sr EXAFS on layered Sr-substituted samples, to provide important angle information. Polarized EXAFS involves collecting spectra for different incident angles ($\theta$) between the membrane normal of the layered sample and the X-ray electric field vector. Dichroism in the EXAFS can occur, depending on how the particular absorber–backscatterer (A–B) vector is aligned with the electric field. Through analysis of the dichroism, we extract the average orientation ($\phi$) of this A–B vector relative to the membrane normal, and the average number of scatterers per absorbing atom ($N_{iso}$). Constraints on the structural model are then imposed by these parameters.

In a complementary and definitive experiment, we use Ca K-edge EXAFS studies to probe the binding site of the native cofactor for any nearby Mn, within ~ 4 Å. This is analogous to the Sr EXAFS studies already published (Cinco et al., 1998), but it focuses on the native cofactor and avoids the treatments involving Ca depletion and Sr substitution. The samples examined were PS II membrane particles from spinach. This new technique promises to be a more sensitive and direct probe of the calcium binding site in PS II than Sr EXAFS. Clarifying whether the Ca cofactor is proximate to the Mn cluster, and finding its coordination environment at the various intermediate S-states of the OEC will reveal its important role in oxygen evolution.

## Materials and Methods

Procedures for the polarized Sr EXAFS experiment have been detailed in an earlier report (Cinco, 1999) and will be summarized briefly. Sr-substituted PS II samples were made by a process of Ca depletion, $Sr^{2+}$ reactivation, and Chelex treatment to remove excess Sr (Cinco et al., 1998). Samples were assayed for oxygen-evolving activity, metals quantitation (Mn and Sr) and EPR multiline signal generation (from the $S_2$ state). Oriented samples were made by layering onto flat Mylar films (Dau et al., 1995). We estimated the degree of disorder (mosaic spread) inherent in the layered samples to be 15 ± 5° by EPR methods (Mukerji et al., 1994). Following the previous Sr EXAFS report (Cinco et al., 1998), EXAFS spectra were collected on Sr-PS II multilayers at several angles between the X-ray electric field vector and the substrate normal ($\theta$ = 10°, 30°, 45°, 70° and 80°). Six separate samples were used, with at least two angles per sample for a total of 15 separate data points. Data analysis was done as described elsewhere (Cinco, 1999); to evaluate the linear dichroism of the Sr EXAFS and find the relative orientation of the vector of interest ($\phi$), we used the formalism of Dittmer and Dau (1998). To a first approximation, there is a $\cos^2$-dependence of the EXAFS on the angle between the X-ray electric field vector and the absorber-scatterer vector of interest.

For the Ca EXAFS experiment, we started with PS II-enriched membranes from spinach (BBY particles). Direct Chelex resin treatment of PS II (Han & Katoh, 1993) removed adventitious, weakly-bound Ca, then oxygen evolution and the EPR multiline signal were assayed. The method has been shown to reduce the Ca content to 2 Ca per PS II. Chelex-treated PS II was accumulated on the flat surface of solid Plexiglas (Ca-free) through seven paint-and-dry cycles, in cold (4°C) and dark conditions and under a stream of dinitrogen (Mukerji et al., 1994; Dau et al., 1995). Dark adaptation throughout the process poised the samples in the $S_1$ state. To prepare the parallel control (inactive) sample, 40 µL of hydroxylamine ($NH_2OH$, 100 mM) was added to the surface of the layered PS II, was allowed to soak and dry without loss of PS II material. Ca EXAFS experiments were done at SSRL beamline IV-2 at the Ca K-edge (4.05 keV) using a modified liquid-He flow cryostat and a Ge detector. A He flight path was also installed to maximize incident X-ray flux. The cryostat setup was designed by Karen McFarlane and incorporated thin (13 – 50 µm) Ca-free Kapton windows that allowed transmission of 4 keV incident X-rays and 3.6 keV fluorescent X-rays. The temperature was maintained at 100 ± 2 K for data collection. EXAFS data were recorded

as fluorescence excitation spectra as the incident X-ray energy was scanned from 4.0 to 4.6 keV using a Si[111] monochromator. Data analysis followed the procedure done for Sr EXAFS (Cinco et al., 1998) but using $E_0$ = 4.05 keV and $k$ range from 2.5 Å$^{-1}$ to 10.5 Å$^{-1}$. Background was removed as a five-domain cubic spline in $k$-space.

## Results

The Fourier transforms from the polarized Sr EXAFS showed extreme dichroism in peak II (Figure 2). Among the excitation angles studied ($\theta$), peak II had the largest magnitude at 10° and smallest at 80°. The other intermediate angles (30° and 45°) had intermediate magnitudes (not shown). Peak II from $\theta$ = 10°, 30° and 45° was Fourier-isolated and simulated with one shell of Mn scatterers, because carbon and other light atoms were previously ruled out as possible scatterers (Cinco et al., 1998; Cinco, 1999). From the Fourier isolates at each angle, we extracted the apparent coordination number ($N_{app}$) while leaving the Debye-Waller factor ($\sigma^2$) fixed. For the higher angles (70° and 80°), we estimated the $N_{app}$ from the peak heights in the Fourier transforms (comparing peak II at 10° and 80° from the same sample).

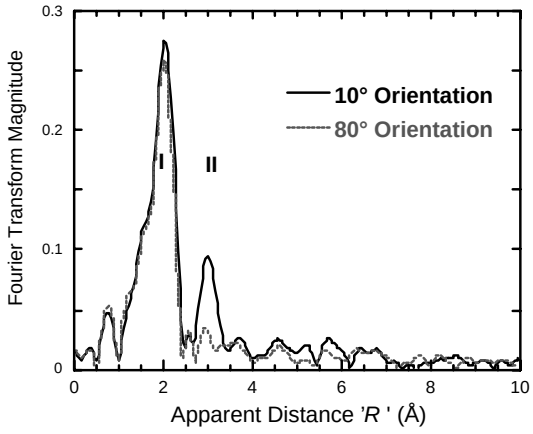


**Fig. 2**. Fourier transforms of $k^3$-weighted EXAFS ($k$ = 2.7 – 11.7 Å$^{-1}$) from oriented Sr-PS II samples at two orientations ($\theta$) between the membrane normal and the X-ray electric field vector. Each trace is averaged from 5 separate samples, with 190 total scans for the 10° spectrum and 160 scans at 80°. The dichroism is most readily apparent in Fourier peak II ('$R$' = 3.0 Å), where the amplitude is largest at 10°, and smallest at 80°. '$R$' is less than the actual distance by about 0.5 Å.

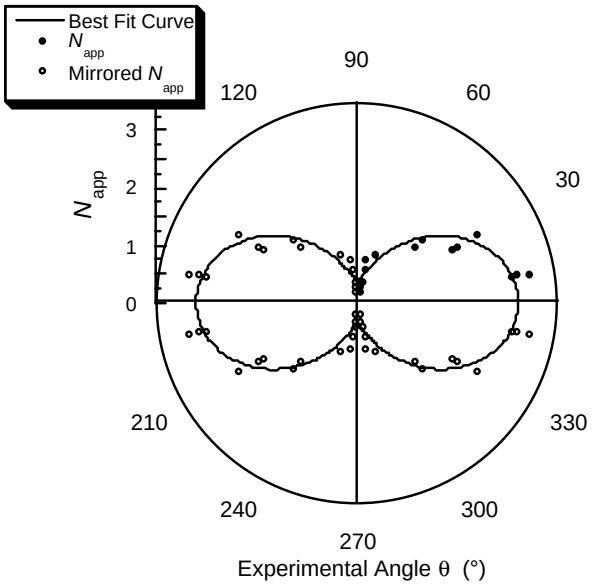


**Fig. 3**. Polar plot of the X-ray absorption linear dichroism from oriented Sr-PS II samples. The various $N_{app}$ derived from EXAFS curve fitting are plotted as radial distances (solid circles) with their respective detection angles $\theta$. A best fit of $N_{app}$ vs. $\theta$ is shown as the solid curve simulating $N_{iso}$ = 1.2 ± 0.3 Mn and $\phi$ = 23 ± 4°. The data points (open circles) and fit between 90° and 360° are mirrored from the $\theta$ = 0°– 90° region.

With $N_{app}$ found for each excitation angle, $\theta$, we plotted these values in a polar plot (Dau et al., 1995; Dittmer & Dau, 1998) to find the relative orientation ($\phi$) of the Sr–Mn vector and its isotropic coordination number $N_{iso}$. Nonlinear least-squares regression analysis produced the solid curve shown in Figure 3 as the best fit of the 15 data points (angles from six separate samples): $\phi$ = 23 ± 4° and $N_{iso}$ = 1.2 ± 0.3. This result translates to 1–2 Sr–Mn vectors with an average angle of 23 ± 4° from the membrane normal.

The Chelex treatment reduced the amount of Ca to 2 Ca/4 Mn/PS II (250 Chl) while not affecting oxygen-evolving activity or the $S_2$ EPR multiline signal. The Ca EXAFS experiment probed the two Ca present

in oxygen-evolving PS II membranes, but of these, only one $Ca^{2+}$ is involved in oxygen evolution (Han & Katoh, 1993). The Fourier transform of the Ca EXAFS is presented in Figure 4 ($k$ range = 2.5 – 10.5 $Å^{-1}$). Each spectrum represents the average of at least 130 scans from three separate samples. The spectra are remarkably similar to the Fourier transforms of the parallel, earlier Sr EXAFS study with Sr substituted for Ca (Fig. 1). The first (largest) Fourier peak corresponds to the coordinating oxygen atoms closest to calcium. In contrast to the control ($NH_2OH$-treated) sample, the Chelex-treated PS II shows a second Fourier peak near 'R' ~ 2.9 Å. When this peak II is isolated and simulated with possible scattering atoms, it fit best to Mn at 3.4 Å, rather than to light atom (C, O or Cl) neighbors. These results were consistent with the parallel, earlier Sr EXAFS studies (Figs. 1 and 2) (Cinco et al., 1998).

## Discussion

The observed dichroism and the curve fitting of Fourier peak II in the polarized Sr EXAFS further support the previous finding that Mn is within 3.5 Å for the Sr cofactor (Cinco et al., 1998). If many (> 2) light atoms such as C or O accounted for Fourier peak II, such a marked dichroism (Fig. 2) would be virtually impossible. It would be difficult to align 3 – 4 (or more) vectors parallel or perpendicular with the X-ray electric field vector to produce the observed behavior. Analysis of the pronounced dichroism in the Sr EXAFS (Fig. 3), yields the relative orientation ($\phi$) of the Sr–Mn vectors as 23 ± 4° and $N_{iso}$ as 1.2 ± 0.3. We believe this result for $N_{iso}$ is consistent with the earlier finding of 2 Sr–Mn vectors from Sr EXAFS studies on isotropic (randomly oriented) PS II samples (Cinco et al., 1998). The new information from polarized Sr EXAFS is the average orientation of 23 ± 4° around the membrane normal.

The more difficult experiment using Ca EXAFS has again detected Mn proximate to the Ca cofactor, within 3.4 Å. The shorter distance agrees with the smaller radius of the $Ca^{2+}$ compared to $Sr^{2+}$ (0.1 Å smaller). Further studies are underway to verify the exact number of Ca–Mn vectors. Nevertheless, this result provides proof of the Mn/Ca heteronuclear cluster as the catalytic site of oxygen evolution in Photosystem II. The Ca EXAFS protocol has directly probed the Ca cofactor in its native state, avoiding potentially disruptive treatments such as the low pH exposure involved in metal substitution. The validation of the proximity of Ca to Mn should stimulate questions and further studies on the actual role of calcium in oxygen evolution.

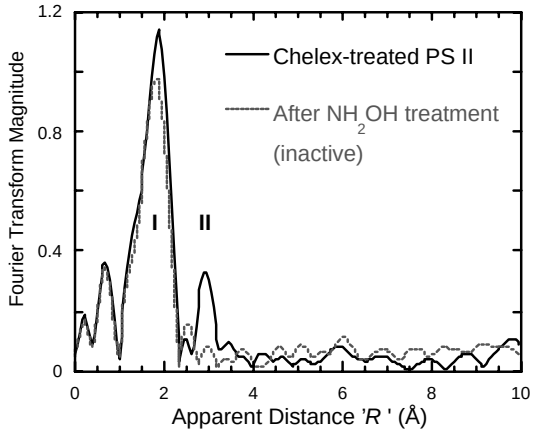


**Fig. 4.** Fourier Transform of Ca EXAFS from Chelex-treated, layered samples with 2 Ca/PS II ($k^3$-weighted, $k$ = 2.5–10.5 $Å^{-1}$). The feature at '$R$' = 0.7 Å is an artifact due to incomplete background removal. '$R$' is smaller than the actual distance by about 0.5 Å.

The orientation data from the Sr EXAFS experiments can be combined with the dichroism data from Mn EXAFS data to calculate the orientation of the 3.3 Å Mn–Mn vector. Fourier Peak III in the Mn EXAFS which contains Mn–Mn (3.3 Å) and Mn–Ca (3.4 Å) contributions, is dichroic, with an average angle of 43 ± 10° with respect to the membrane normal (Mukerji et al., 1994). Moreover, the 43 ± 10° estimate is a $\cos^2\phi$-weighted average of the orientations of the Mn–Mn (3.3 Å) and the Mn–Ca vectors. (Dau et al., 1995). After solving for the Mn–Mn contribution to the average, our finding from the polarized Sr EXAFS experiments that the Mn–Ca angle is ~ 23° leads to an alignment of ~ 62° for the 3.3 Å Mn–Mn vector. Previous polarized Mn EXAFS experiments on PS II have shown angles of 55° and 67° for the two

2.7 Å Mn–Mn vectors (Mukerji et al., 1994; Dau et al., 1995). All three Mn–Mn vectors then lie at roughly the same angle with respect to the membrane plane, but are not restricted to being collinear, because the PS II membranes are ordered in one dimension only.
Because significant angle information about Mn–Mn and Mn–Ca vectors is now available, other topological models previously discussed (DeRose et al., 1994) can be refined to include the presence of Ca and account for the dichroism data. Three possible refined models are presented in Figure 5. Recent EXAFS data from the $S_0$ state has indicated that there maybe three di-μ-oxo bridged Mn-Mn units. Models based on that data are presented by Robblee et al. in this issue. However, such motifs were not included in Figure 5, but considering them is a subject for future work.

Polarized Sr EXAFS on oriented samples has obtained important angle information about the calcium cofactor to refine the model for the OEC of PS II, while Ca EXAFS provided direct proof of Mn proximity to the cofactor. Taken together, the evidence presented clearly reinforces the concept of a Mn/Ca heteronuclear cluster as the catalytic center of the water oxidation.

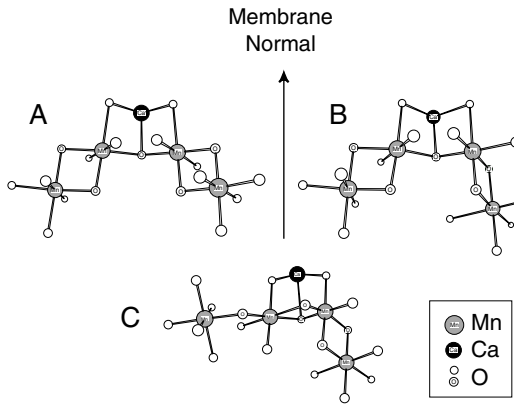


**Fig. 5.** Refined models for the active site of the OEC in Photosystem II. These models combine the finding from oriented Sr-substituted PS II samples with previous results from Mn EXAFS on oriented PS II samples.These are derived from core structures that have been described in earlier studies (Fig. 5A-B from option A and Fig. 5C from option F in DeRose et al., 1994).

## Acknowledgments

This research was supported by the National Institutes of Health Grant (GM-55302), and the Director, Office of Science, Office of Basic Energy Sciences, Division of Energy Biosciences, U. S. Department of Energy under contract DE-AC03-76SF00098. Synchrotron radiation facilities were provided by the Stanford Synchrotron Radiation Laboratory which is operated by the DOE, Office of Basic Energy Sciences. SSRL Biotechnology Program is supported by the NIH, National Center of Research Resources, Biomedical Technology Program, and by the DOE, Office of Biological and Environmental Research. JM thanks the DFG grants Me1629/1-1, 2-1 and 2-2 for support. RMC thanks the Ford Foundation for a predoctoral fellowship.

## References

Boussac A, Rutherford AW (1988) *Biochemistry* **27**, 3476-3483.
Cinco RM (1999) Ph.D. Dissertation, University of California, Berkeley, LBNL-44753.
Cinco RM, Robblee JH, Rompel A, Fernandez C, Yachandra VK, Sauer K, Klein MP (1998) *Journal of Physical Chemistry B* **102**, 8248-8256.
Dau H, Andrews JC, Roelofs TA, Latimer MJ, Liang W, Yachandra VK, Sauer K, Klein MP (1995) *Biochemistry* **34**, 5274-5287.
Debus RJ (1992) *Biochimica et Biophysica Acta* **1102**, 269-352.
DeRose VJ, Mukerji I, Latimer MJ, Yachandra VK, Sauer K, Klein MP (1994) *Journal of the American Chemical Society* **116**, 5239-5249.
Dittmer J, Dau H (1998) *Journal of Physical Chemistry B* **102**, 8196-8200.
Han K-C, Katoh S (1993) *Plant & Cell Physiology* **34**, 585-593.

Latimer MJ, DeRose VJ, Mukerji I, Yachandra VK, Sauer K, Klein MP (1995) *Biochemistry* **34**, 10898-10909.

Mukerji I, Andrews JC, DeRose VJ, Latimer MJ, Yachandra VK, Sauer K, Klein MP (1994) *Biochemistry* **33**, 9712-21.

Riggs-Gelasco PJ, Mei R, Ghanotakis DF, Yocum CF, Penner-Hahn JE (1996) *Journal of the American Chemical Society* **118**, 2400-2410.

Robblee JH, Cinco RM, Yachandra VK (2001) *Biochimica et Biophysica Acta* **1503**, 7-23.